



Article

Summer Monsoon Season Streamflow Variations in the Middle Yellow River since 1570 CE Inferred from Tree Rings of *Pinus tabulaeformis*

Feng Chen ^{1,2,*}, Magdalena Opala-Owczarek ³ , Piotr Owczarek ⁴  and Youping Chen ¹

¹ Yunnan Key Laboratory of International Rivers and Transboundary Eco-Security, Institute of International Rivers and Eco-Security, Yunnan University, Kunming 650500, China; 20190012@ynu.edu.cn

² Key Laboratory of Tree-ring Physical and Chemical Research of China Meteorological Administration/Xinjiang Laboratory of Tree-Ring Ecology, Institute of Desert Meteorology, China Meteorological Administration, Urumqi 830002, China

³ Institute of Earth Sciences, Faculty of Natural Sciences, University of Silesia in Katowice, Ul. Bedzinska 60, 41-200 Sosnowiec, Poland; magdalena.opala@us.edu.pl

⁴ Institute of Geography and Regional Development, University of Wrocław, Pl.Uniwersytecki 1, 50-137 Wrocław, Poland; piotr.owczarek@uwr.edu.pl

* Correspondence: feng653@ynu.edu.cn

Received: 25 April 2020; Accepted: 3 July 2020; Published: 6 July 2020



Abstract: This study investigates the potential reconstruction of summer monsoon season streamflow variations in the middle reaches of the Yellow River from tree rings in the Qinling Mountains. The regional chronology is significantly positively correlated with the July–October streamflow of the middle Yellow River from 1919 to 1949, and the derived reconstruction explains 36.4% of the actual streamflow variance during this period. High streamflows occurred during 1644–1757, 1795–1806, 1818–1833, 1882–1900, 1909–1920 and 1933–1963. Low streamflows occurred during 1570–1643, 1758–1794, 1807–1817, 1834–1868, 1921–1932 and 1964–2012. High and low streamflow intervals also correspond well to the East Asian summer monsoon (EASM) intensity. Some negative correlations of our streamflow reconstruction with Indo-Pacific sea surface temperature (SST) also suggest the linkage of regional streamflow changes to the Asian summer monsoon circulation. Although climate change has some important effects on the variation in streamflow, anthropogenic activities are the primary factors mediating the flow cessation of the Yellow River, based on streamflow reconstruction.

Keywords: Yellow River; tree rings; streamflow reconstruction; East Asian summer monsoon; climate warming

1. Introduction

Hydrological changes and their associated water resources are closely related to society in China [1,2]. Hydrology-related natural disasters, such as floods and prolonged drought, can translate into infrastructure destruction and the loss of industrial and agricultural production, and have serious economic and social impacts. These impacts could seriously threaten the lifestyles of human beings in river basins in China. With the rapid increase in water consumption in China over the past 30 years and the high uncertainty of future water resource change in the context of global warming [3–6], reliable knowledge of streamflow variations is of importance for us to assess the spatial-temporal variation in water resources in river basins and remote areas. Long-term and high resolution dendrohydrological reconstructions provide important contributions to the body of knowledge on past hydrological variations and can facilitate efforts to simulate future hydrological scenarios [7–12].

The Yellow River, one of the longest river systems in the world and the second longest in China, provides abundant freshwater for the people living along the river. In the Yellow River basin, some annually resolved series (12 months) of natural streamflow were reconstructed during the last millennium, based on tree-ring data from the Tibetan Plateau [13,14]. Most of these reconstructions are based on the response of tree-ring width to the streamflow of water years. Summer monsoon season streamflow records in the middle Yellow River, however, rarely extend beyond the Little Ice Age and contain relatively weak hydrological signals [15–17]. Some studies have proven the sensitivity of tree rings of Chinese pine (*Pinus tabulaeformis*) to summer monsoon season streamflow in the middle Yellow River basin [18–21]. The dendrohydrological potential of Chinese pine, however, depends on a convincing separation of naturally and anthropogenically induced streamflow signals at different time scales [14].

This research focused on developing a regional chronology and extracting streamflow signals based on the tree rings of *P. tabulaeformis* at three sampling sites (SR, XF and NWT) [20,22,23] in the Qinling Mountains (Figure 1 and Table 1) and presented a streamflow reconstruction that overcomes some of these restrictions, linked with streamflow sensitivity and anthropogenic influence, to reconstruct summer monsoon season streamflow variations in the middle Yellow River since 1570 CE. Therefore, we compiled a regional tree-ring width chronology based on tree-ring data from three sampling sites in the middle reaches of the Yellow River, Central China. We attempted to show high to low frequency streamflow signals of the new streamflow reconstruction and discuss the effects of synoptic variations on streamflow according to the new streamflow reconstruction and other findings available from adjacent regions.

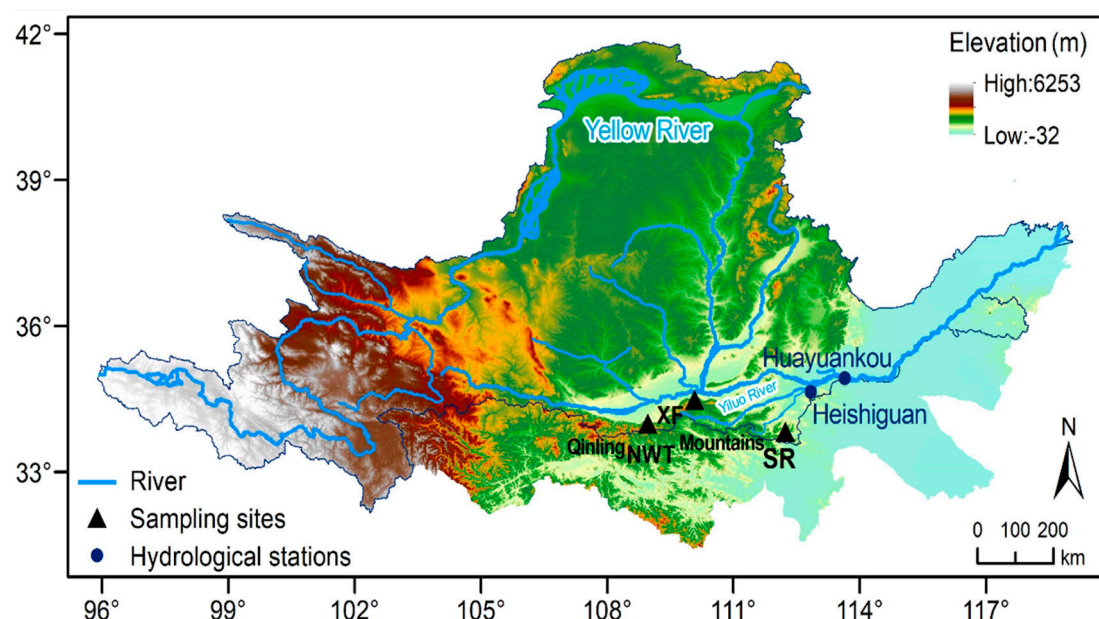


Figure 1. Map showing the locations of sampling sites and hydrological stations in the middle reaches of the Yellow River.

Table 1. Site information for tree-ring width chronologies and hydrological stations in the middle Yellow River basin.

Site Code	Latitude (N)	Longitude (E)	Number of Trees /Sample Depth	Elevation (m)	Species	Time Span (CE)
XF	34°29′	110°05′	25/51	2030–2050	<i>P. tabulaeformis</i>	1543–2012
NWT	34°00′	108°58′	25/51	1380–1450	<i>P. tabulaeformis</i>	1795–2010
SR	33°44′	112°14′	29/57	1675	<i>P. tabulaeformis</i>	1774–2007
Huayuankou	34°55′	113°39′	-	92	-	1919–1988
Heishiguan	34°43′	112°56′	-	109	-	1950–1986

2. Material and Methods

2.1. Geographical Settings and Tree-Ring Material

The study areas are situated in Central China with typical monsoon climate characteristics in a humid and semi-humid climatic zone (Figure 1). The annual total precipitation is approximately 633.5 mm, and the annual average temperature is 12.5 °C, based on monthly climate datasets of the Climatic Research Unit (CRU) of the University of East Anglia (averaged over 33.5–36° N, 109–114° E, [24]). Under the influence of the Asian monsoon, the summer climate of the study region is hot and rainy, while the winter climate is dry and cold and controlled by dry-cold airflows from high latitudes (Figure 2a). The mean annual streamflow of the Yellow River (34°55′ N, 113°39′ E, 92 m a.s.l.) at the Huayuankou hydrological station is 1436 m³/s during the period 1919–1988. Figure 2b indicates the monthly average streamflow of the middle Yellow River from 1919 to 1988, and the seasonal distributions of streamflow and precipitation are highly similar. The streamflows increase rapidly during summer, along with increases in monsoon precipitation. The Qinling Mountains are the most important orographic barrier in the study area and serve as the dividing line between northern and southern China. As a dominant tree species in the Qinling Mountains, Chinese pines grow on thin or rocky soils on the peaks of mountains and are known to be strongly sensitive to climatic change and are significantly positively correlated with streamflow and precipitation variations over a broad area in Central China [19–23]. This research attempted to develop a regional chronology and to reconstruct the streamflow of the Yellow River based on the tree rings of Chinese pines from three sampling sites (SR, XF and NWT) [20,22,23] located in the Qinling Mountains (Figure 1 and Table 1).

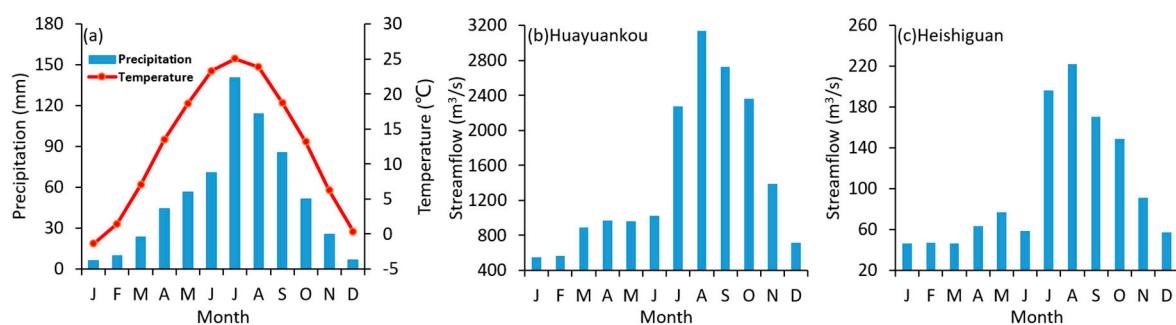


Figure 2. (a) Average monthly precipitation and temperature of the middle reaches of the Yellow River from 1950 to 2018, based on monthly climate datasets of the Climatic Research Unit (CRU) of the University of East Anglia (averaged over 33.5–36° N, 109–114° E). (b) The average monthly streamflow from 1919 to 1988 at the Huayuankou hydrological station. (c) The average monthly streamflow from 1951 to 1986 at the Heishiguan hydrological station.

Significant common signals among the individual ring-width series were confirmed by cross-dating. To remove nonclimatic trends, negative exponential or straight-line curve fits were used. After detrending with the negative exponential curve, all individual ring-width sequences from the three sampling sites were merged into a regional chronology (RC) using a bi-weight robust mean in the ARSTAN program [25]. The bi-weight robust mean minimizes the effect of outliers, extreme values or biases in the tree-ring index. The correlation analysis revealed that high correlations existed between the site chronologies, and the regional chronology displayed significant common signals (Table 2). To capture the low to high frequency common variance, the standard version (STD) of the regional chronology was used in the streamflow reconstruction. The reliability of the regional chronology was assessed by the expressed population signal (EPS) and interseries correlation (Rbar) [26]. Both Rbar and EPS were computed over 50 years, lagged by 25 years. To minimize the influence of changing sample depth, the variance in the regional chronology was stabilized using methods shown by Osborn et al. [27].

Table 2. Correlations among the tree-ring width chronologies during the common period 1850–2007.

	SR	XF	NWT
SR	1.00 *		
XF	0.47 *	1.00 *	
NWT	0.25 *	0.53 *	1.00 *
RC	0.71 *	0.83 *	0.79 *

* indicates 99% confidence level.

2.2. Streamflow Data and Analyses

We selected two hydrological stations near the sampling sites in the study area: Huanyuankou station in the Yellow River (34°55′ N, 113°39′ E, 92 m a.s.l., observation period 1919–1988) (Figure 2b) and Heishiguan station in the Yiluo River (34°43′ N, 112°56′ E, 109 m a.s.l., observation period 1951–1986) (Figure 2c). The monthly mean streamflow of each station was calculated. Clearly, in the middle sections of the Yellow River, high summer monsoon precipitation coincides with high streamflow during July to September, and in contrast, this area is controlled by a cold dry air mass in winter (Figure 2). In Pearson’s correlation analysis, the streamflow data of Huanyuankou and Heishiguan along with the regional chronology were examined from January to December. All statistical procedures were evaluated at the $p < 0.05$ level of significance. Based on the results of the streamflow response, a linear regression equation was used to reconstruct the streamflow variation in the middle Yellow River. Since the calibration period is relatively short, statistical tests, including the reduction of error (RE), Pearson correlation coefficient (r) and coefficient of efficiency (CE), were computed using the method of leave-one-out cross-validation [28]. To establish connections between our streamflow reconstruction and the atmospheric circulations in East Asia, we analyzed multiple correlations of our streamflow reconstruction with the EASM index [29] and sea surface temperature dataset (HadSST2, [30]) for the common period.

3. Results and Discussion

3.1. Streamflow Reconstruction

To guarantee the reliability of the streamflow reconstruction, we truncated the early portion of the regional chronology prior to 1570 based on an expressed population signal of at least 0.85. The moving EPS values from 1570 to 2012 were close to 0.9, further revealing the reliability of the regional chronology. Figure 3 indicates the correlations between the monthly streamflow data and the regional chronology. The tree-ring widths of *P. tabulaeformis* show remarkable ($p < 0.05$) positive correlations with the streamflow of the Yiluo River (Heishiguan) during June–August. Similarly, there were some significant positive correlations between the regional chronology and streamflow of the Yellow River (Huayuankou) during June–December. After screening the regional chronology in correlation analysis with the streamflow combinations from January to December, the strongest correlation ($r = 0.64$, $p < 0.01$) was found between the regional chronology and the June–August streamflow of the Yiluo River, and a high correlation ($r = 0.61$, $p < 0.01$) was found between the regional chronology and the July–October streamflow of the Yiluo River. Moreover, a high correlation of the regional chronology was found for the July–October streamflow of the Yellow River, with $r = 0.42$ ($p < 0.01$). The correlation between the streamflow of Heishiguan and Huayuankou reached 0.70 ($p < 0.01$), despite considerable anthropogenic influences (Figure 4).

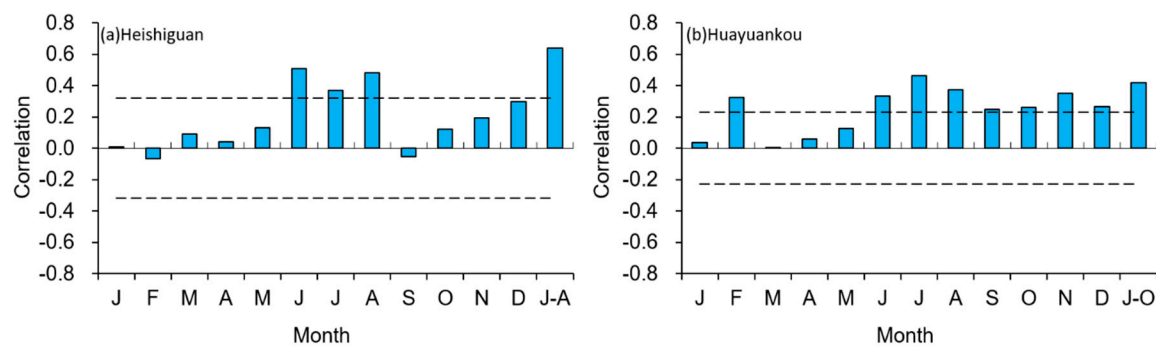


Figure 3. Correlation analyses between the regional chronology and streamflow at Heishiguan (a) and Huayuankou (b). The dashed lines represent the 95% confidence level.

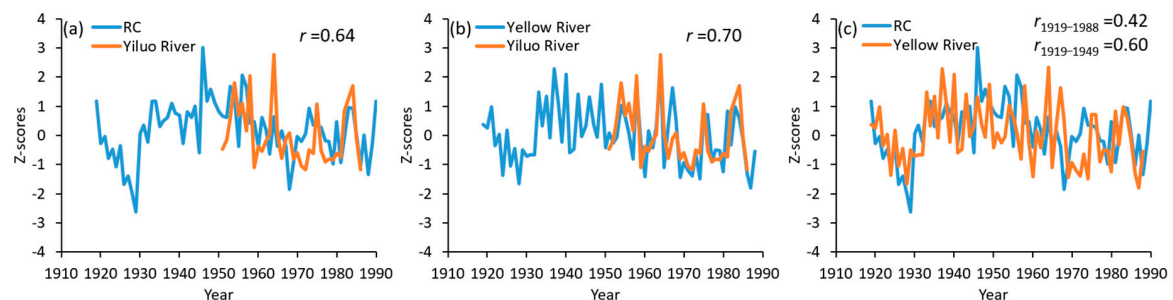


Figure 4. (a) Comparison between the regional chronology (RC) and observed June–August streamflow of the Yiluo River (Heishiguan). (b) Comparison between the July–October streamflow of the Yellow River (Huayuankou) and the July–October streamflow of the Yiluo River (Heishiguan). (c) Comparison between the regional chronology (RC) and the observed July–October streamflow of the Yellow River (Huayuankou).

First, a linear regression equation was established to reconstruct the streamflow history for the Yiluo River. During the common period of the regional chronology and streamflow data (1951–1986), the streamflow reconstruction accounted for 41% of the actual streamflow variance (Figure 4a). Although this reconstruction is statistically stable, we found that streamflow in July 1958 was unusual, related to the maximum flow recorded during the instrumental period. If we eliminated 1958 from the reconstruction equation, the explained variance increases from 41% to 48%. Considering that the Yiluo River is a tributary of the Yellow River and the river basin is located in the Qinling Mountains with less human disturbances, the instrumental streamflow data of this river provide a reference to validate our streamflow reconstruction of the Yellow River. To a certain extent, the regional chronology can also represent the changes in the natural streamflow in this region after the 1950s, as indicated by the results.

Since the 1950s, a large number of hydraulic engineering structures have been built in the middle reaches of the Yellow River, and the response of tree rings to streamflow has been considerably reduced due to strong anthropogenic influences [14]. Although the correlation was high during the entire period of 1919–1988, the correlation between the July–October streamflow of the Yellow River and the regional chronology was just 0.28 ($p < 0.10$) during the period 1950–1988, which also indicates that the streamflow variation in this area is seriously influenced by anthropogenic factors. The first-differenced correlation from 1950 to 1988 is $r = 0.07$ ($p > 0.01$), indicating that low frequency variation is relatively coherent between the regional chronology and observed streamflow data. The instrumental streamflow data are 9.7% less than the reconstructed streamflow data, and the anthropogenic influence is even stronger in the last 30 years [14]. It is believed that the streamflow in the middle Yellow River is influenced by the fluvial processes in its upper reaches, such as the Tibetan Plateau, and by the streamflow from the Qinling Mountains; thus, a strong correlation ($r = 0.70$, $p < 0.01$) between the streamflow of Heishiguan and Huayuankou was found, despite considerable anthropogenic influences (Figure 4b). Therefore,

the tree-ring width chronologies of *P. tabulaeformis*, which are sensitive to the streamflow variation in the Qinling Mountains and were utilized as a proxy to reconstruct the hydrological variables of the Yiluo River, may also be used to acquire the streamflow signals of the middle Yellow River. Detailed analysis indicated that a high correlation ($r = 0.60$, $p < 0.01$) was found between the regional chronology and the July–October streamflow of the Yellow River and affected the changes in subsequent streamflow. The reconstruction equation between the July–October streamflow of the Yellow River and the regional chronology achieved reliable calibration and cross-validation statistics. The final calibration regression ($Y = 3462.699RC - 775.865$) explained 36.4% of the total variance of the instrumental streamflow during 1919–1949 (Figure 4c) and 33.6% in the leave-one-out cross-validation. The positive CE (0.27) and RE (0.28) revealed the good predictive skill of the reconstruction equation.

Figure 5a exhibits the interannual to multidecadal variability of the July–October streamflow reconstruction for the middle Yellow River since 1570 CE. Several extended high and low streamflow epochs (≥ 11 years) were revealed according to 25-year low pass filtered streamflow values of the reconstruction and the long-term mean (1570–2012, $2670.6 \text{ m}^3/\text{s}$). Low streamflow epochs occurred around 1570–1643, 1758–1794, 1807–1817, 1834–1868, 1921–1932 and 1964–2012, while high streamflow periods occurred at 1644–1757, 1795–1806, 1818–1833, 1882–1900, 1909–1920 and 1933–1963. The streamflows less than the mean- 1σ ($2166.8 \text{ m}^3/\text{s}$) for three or more consecutive years occurred at 1576–1580, 1632–1635 and 1926–1929, and conversely, the streamflows higher than the mean+ 1σ ($3174.4 \text{ m}^3/\text{s}$) for three or more consecutive years occurred at 1675–1678, 1747–1749, 1803–1806, 1894–1898 and 1946–1949. A trend towards decreased streamflow begins in the middle of the 20th century and continues into the 21st century.

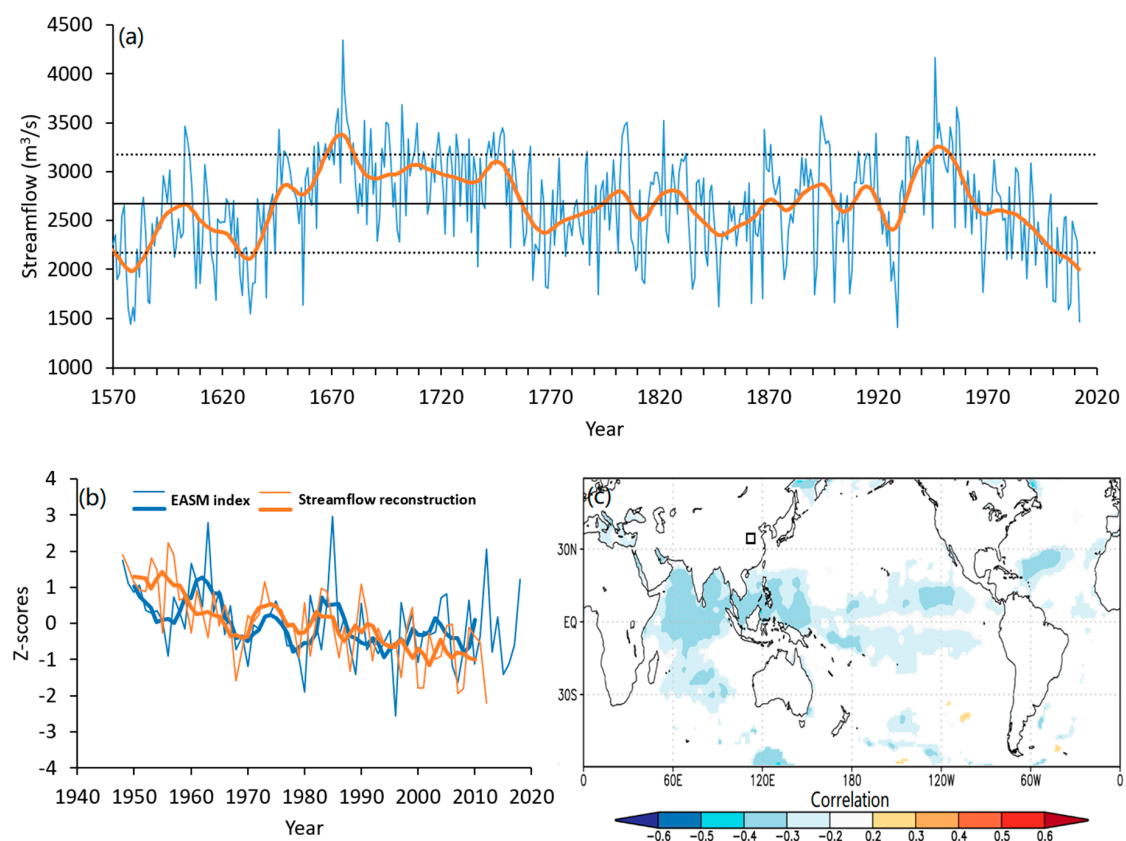


Figure 5. (a) Estimated (thin line) and 25-year low pass filter (thick line) values of the July–October streamflow of the Yellow River. The central horizontal line shows the mean of the estimated values; the dotted lines show the border of one standard deviation. (b) Comparison between the July–October streamflow reconstruction of the Yellow River and the EASM over the 1948–2012 period. (c) Correlation patterns of the reconstructed streamflow with the July–October Indo-Pacific SSTs over the 1870–2012 period.

3.2. Link with the East Asian Summer Monsoon (EASM) and the Indo-Pacific Ocean Climate

Commonly, with the northward movement of the monsoon rain belt, the middle Yellow River is substantially impacted by the EASM during June to October, and monsoon precipitation and streamflow increase rapidly, especially the July streamflow (Figure 2). The instrumental climate data show that the total precipitation and streamflow from June to October account for 73% of the annual precipitation and 66% of the annual streamflow in the middle Yellow River basin, respectively. The correlation between the observed precipitation and streamflow from 1953 to 1988 is $r = 0.60$ ($p < 0.01$). The EASM intensity is indicated by streamflow to a certain degree. Thus, it is obvious that the streamflow variation in this region is closely linked to the intensity of the East Asian summer monsoon and its associated monsoon precipitation [31]. In other words, higher streamflows mean a stronger summer monsoon, and vice versa. Based on the above points, the low and high streamflow periods correspond to weak and strong summer monsoon intervals, respectively. To establish the linkages between our streamflow reconstruction and the EASM, we analyzed the correlations between the EASM index and our streamflow reconstruction [29] for the 1948–2012 period. The stronger correlation ($r = 0.23$, $p = 0.06$) was between the concurrent June EASM index and our streamflow reconstruction and increased to 0.56 ($p < 0.01$) after 5-point smoothing (Figure 5b). Although we do not want to overinterpret these weak correlations, the positive correlations with the EASM index also suggest that the water cycles of the middle Yellow River are linked closely with the East Asian summer monsoon dynamics, which affect precipitation conditions over the Qinling Mountains [32–34]. This result is in line with our expectations.

As shown in Figure 5c, some significant negative correlation areas with SSTs were found in the northern Indian Ocean and western tropical Pacific Ocean, implying that these tropical sea areas are the main water vapor sources for the middle Yellow River. Hydroclimatic conditions in Central China would be impacted by the Asian summer monsoon through water vapor transport from sea areas around China [29,35]. These water vapor source areas influenced by the Asian summer monsoon [36,37] also suggest possible teleconnections between our streamflow reconstruction and the Asian summer monsoon systems. Significant negative correlations between the moisture-sensitive tree-ring width record and SSTs in the northern Indian Ocean and western tropical Pacific Ocean are also found in the neighboring area [36], suggesting similar hydroclimatic variations for both areas. Although instrumental climatic data showed that the EASM has significantly weakened since the 1970s [29,38], our reconstruction shows that this dry trend may have started after the warm 1940s. During the past 30 years, this downward trend has been further exacerbated by increased evaporation as a result of climate warming [39], despite the EASM recovering from its weak epoch since the 1990s [40].

3.3. Human Impacts

The sampling sites used in our streamflow reconstruction in this study are relatively dry, and therefore, these pine trees have suffered from water stress during the warm period [20,22,23]. Warm season temperature increases during recent years could have contributed to increasing water scarcity in the Yellow River [39]. The temperature increase since the 1980s, shown by tree-ring records [21,41] as a period of unusual warm temperatures, could have exacerbated the recent drought across the middle Yellow River basin. At the same time, we found that there is a significant negative correlation ($r = -0.31$, $p < 0.01$) between the low frequency variations in the annual streamflow reconstruction [14] and our seasonal streamflow reconstruction (Figure 6), which may suggest that the increase in runoff caused by increased melting of snow and ice in the Tibetan Plateau under the background of climate warming cannot completely offset the decrease in runoff caused by increasing water consumption and warming-induced drought downstream. The recent drought trend, by influencing available water resources and water cycles, was also one of the contributing factors to the flow cessation events of the Yellow River that occurred in the 1990s [42,43], especially for the drought year 1997 [36]. This region is the most important grain production area in China, and as a

result of rapid socioeconomic development, regional water consumption has rapidly increased, and the influences of human actions on the streamflow of the Yellow River are further strengthening [14]. As shown by our streamflow reconstruction, severe low runoff periods in history that coincided with drought events occurred in the middle reaches of the Yellow River, especially in the late Ming Dynasty (1620–1644), 1877–1878 and 1926–1929, causing environmental and social impacts [44–46] but rarely causing cessation of Yellow River flow. Therefore, modern flow cessation is the product of the superimposed impacts of human activities and contemporary climate change. Although no flow cessation events occurred after the implementation of the reasonable streamflow allocation scheme, a warm climate could increase evaporative demand, and the deleterious influence of climate warming will become considerably more widespread in the future [47–49]. Therefore, for the different future climate scenarios, a reasonable runoff allocation scheme is necessary.

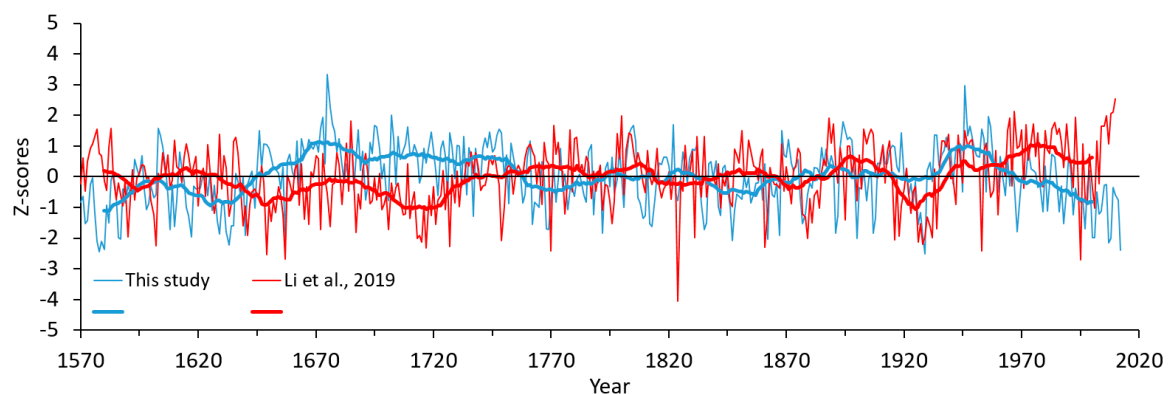


Figure 6. Comparison between the streamflow reconstructions of the Yellow River for the summer monsoon season (July–October, this study) and water year (October–September) [14].

4. Conclusions

The regional chronology of *P. tabulaeformis* was constructed for the Qinling Mountain area, Central China. The streamflow reconstruction was developed for the 1570–1918 period using an equation calibrated with instrumental streamflow of the middle Yellow River. The reconstruction accounted for 36.4% of the variance in the instrumental streamflow over the 1919–1949 period. The reconstruction reflects not only the streamflow fluctuations in the middle Yellow River basin, but also the strong/weak EASM variations. Significant negative correlations of our streamflow reconstruction with Indo-Pacific SSTs imply connections of the middle Yellow River streamflow variation with the Asian summer monsoon system. Under the background of warming-drying in recent decades, streamflow has been continuously decreasing due to recent intense human activity. Although similar low streamflow events have occurred in the past, none of them caused flow cessation events. Therefore, reasonable streamflow allocation is of strong importance for regional sustainable development and the watershed environment.

Author Contributions: Conceived and designed the experiments: F.C. and Y.C. Performed the experiments: F.C. and Y.C. Analyzed the data: F.C. and Y.C. Contributed reagents/materials/analysis tools: F.C., Y.C., M.O.-O., and P.O. Contributed to the writing of the manuscript: F.C., Y.C., M.O.-O., and P.O. All authors have read and agreed to the published version of the manuscript.

Funding: This work was supported by NSFC Project (U1803341), the National Key R&D Program of China (Grant 2018YFA0606401) and National high-level talents special support plan.

Acknowledgments: We thank the Global Runoff Data Centre for providing streamflow data.

Conflicts of Interest: The authors declare that the research was conducted in the absence of any commercial or financial relationships that could be construed as a potential conflict of interest.

References

1. Liu, C.; Xia, J. Water problems and hydrological research in the Yellow River and the Huai and Hai River basins of China. *Hydrol. Process.* **2004**, *18*, 2197–2210. [\[CrossRef\]](#)
2. Du, W.; Fan, Y.; Liu, X.; Park, S.C.; Tang, X. A game-based production operation model for water resource management: An analysis of the South-to-North Water Transfer Project in China. *J. Clean. Prod.* **2019**, *228*, 1482–1493. [\[CrossRef\]](#)
3. Jiang, Y. China's water scarcity. *J. Environ. Manag.* **2009**, *90*, 3185–3196. [\[CrossRef\]](#)
4. Jiang, S.; Wang, J.; Zhao, Y.; Shang, Y.; Gao, X.; Li, H.; Wang, Q.; Zhu, Y. Sustainability of water resources for agriculture considering grain production, trade and consumption in China from 2004 to 2013. *J. Clean. Prod.* **2017**, *149*, 1210–1218. [\[CrossRef\]](#)
5. Zhai, R.; Tao, F. Contributions of climate change and human activities to runoff change in seven typical catchments across China. *Sci. Total Environ.* **2017**, *605*, 219–229. [\[CrossRef\]](#) [\[PubMed\]](#)
6. Liu, J.; Zhang, Q.; Singh, V.P.; Shi, P. Contribution of multiple climatic variables and human activities to streamflow changes across China. *J. Hydrol.* **2017**, *545*, 145–162. [\[CrossRef\]](#)
7. Gou, X.; Chen, F.; Cook, E.; Jacoby, G.; Yang, M.; Li, J. Streamflow variations of the Yellow River over the past 593 years in western China reconstructed from tree rings. *Water Resour. Res.* **2007**, *43*, 4179–4186. [\[CrossRef\]](#)
8. Ho, M.; Lall, U.; Sun, X.; Cook, E.R. Multiscale temporal variability and regional patterns in 555 years of conterminous U.S. streamflow. *Water Resour. Res.* **2017**, *53*, 3047–3066. [\[CrossRef\]](#)
9. Ravindranath, A.; Devineni, N.; Lall, U.; Cook, E.R.; Pederson, G.; Martin, J.; Woodhouse, C. Streamflow Reconstruction in the Upper Missouri River Basin Using a Novel Bayesian Network Model. *Water Resour. Res.* **2019**, *55*, 7694–7716. [\[CrossRef\]](#)
10. Muñoz, A.A.; González-Reyes, A.; Lara, A.; Sauchyn, D.; Christie, D.; Puchi, P.; Urrutia-Jalabert, R.; Toledo-Guerrero, I.; Aguilera-Betti, I.; Mun'do, I.A.; et al. Streamflow variability in the Chilean Temperate-Mediterranean climate transition (35° S–42° S) during the last 400 years inferred from tree-ring records. *Clim. Dyn.* **2016**, *47*, 4051–4066. [\[CrossRef\]](#)
11. Xu, C.; Buckley, B.M.; Promchote, P.; Wang, S.; Pumijumong, N.; An, W.; Sano, M.; Nakatsuka, T.; Guo, Z. Increased Variability of Thailand's Chao Phraya River Peak Season Flow and Its Association with ENSO Variability: Evidence from Tree Ring $\delta^{18}O$. *Geophys. Res. Lett.* **2019**, *46*, 4863–4872. [\[CrossRef\]](#)
12. Woodhouse, C.A.; Pederson, G.T. Investigating Runoff Efficiency in Upper Colorado River Streamflow Over Past Centuries. *Water Resour. Res.* **2018**, *54*, 286–300. [\[CrossRef\]](#)
13. Gou, X.; Deng, Y.; Chen, F.; Yang, M.; Fang, K.; Gao, L.; Yang, T.; Zhang, F. Tree ring based streamflow reconstruction for the Upper Yellow River over the past 1234 years. *Chin. Sci. Bull.* **2010**, *55*, 4179–4186. [\[CrossRef\]](#)
14. Li, J.; Xie, S.-P.; Cook, E.R.; Chen, F.; Shi, J.; Zhang, D.D.; Fang, K.; Gou, X.; Li, T.; Peng, J.; et al. Deciphering Human Contributions to Yellow River Flow Reductions and Downstream Drying Using Centuries-Long Tree Ring Records. *Geophys. Res. Lett.* **2019**, *46*, 898–905. [\[CrossRef\]](#)
15. Kang, L.L.; Wang, Y.Z.; Ma, Y.; Wei, Y.C. Reconstruction of the natural runoff series in recent 523 years at Huayuankou station in Yellow River. *J. Water Resour. Water Eng.* **2008**, *19*, 10–13. (In Chinese)
16. Pan, W.; Zheng, J.; Xiao, L.; Yan, F. The relationship of nature runoff changes in flood-season of middle Yellow River and Yongding River, 1766–2004. *Acta Geogr. Sinica* **2015**, *68*, 975–982. (In Chinese)
17. Pan, W.; Fei, J.; Man, Z.; Zheng, J.; Zhuang, H.; Man, Z. The fluctuation of the beginning time of flood season in North China during AD1766–1911. *Quat. Int.* **2015**, *380*, 377–381. [\[CrossRef\]](#)
18. Sun, J.; Liu, Y.; Wang, Y.; Bao, G.; Sun, B. Tree-ring based runoff reconstruction of the upper Fenhe River basin, North China, since 1799 AD. *Quat. Int.* **2013**, *283*, 117–124. [\[CrossRef\]](#)
19. Liu, N.; Bao, G.; Liu, Y.; Linderholm, H.W. Two Centuries-Long Streamflow Reconstruction Inferred from Tree Rings for the Middle Reaches of the Weihe River in Central China. *Forests* **2019**, *10*, 208. [\[CrossRef\]](#)
20. Shi, J.; Li, J.; Cook, E.R.; Zhang, X.; Lu, H. Growth response of *Pinus tabulaeformis* to climate along an elevation gradient in the eastern Qinling Mountains, central China. *Clim. Res.* **2012**, *53*, 157–167. [\[CrossRef\]](#)
21. Liu, Y.; Wang, Y.; Li, Q.; Song, H.; Linderholm, H.W.; Leavitt, S.W.; Wang, R.; An, Z.; Linderholm, H.W. Tree-ring stable carbon isotope-based May–July temperature reconstruction over Nanwutai, China, for the past century and its record of 20th century warming. *Quat. Sci. Rev.* **2014**, *93*, 67–76. [\[CrossRef\]](#)

22. Chen, F.; Yuan, Y.; Wei, W.; Fan, Z.; Zhang, R.; Yu, S. April–June precipitation reconstruction for Xi’an and drought assessment for the Guanzhong Plain from tree rings of Chinese pine. *J. Water Clim. Chang.* **2014**, *6*, 638–646. [\[CrossRef\]](#)
23. Chen, F.; Zhang, R.; Wang, H.; Qin, L.; Yuan, Y. Updated precipitation reconstruction (AD 1482–2012) for Huashan, north-central China. *Theor. Appl. Climatol.* **2016**, *123*, 723–732. [\[CrossRef\]](#)
24. Harris, I.; Jones, P.; Osborn, T.J.; Lister, D.H. Updated high-resolution grids of monthly climatic observations - the CRU TS3.10 Dataset. *Int. J. Clim.* **2013**, *34*, 623–642. [\[CrossRef\]](#)
25. Yamaguchi, D.K.; Cook, E.R.; Kairiukstis, L.A. Methods of Dendrochronology, Applications in the Environmental Sciences. *Arct. Alp. Res.* **1991**, *23*, 120. [\[CrossRef\]](#)
26. Fritts, H.C. *Tree-Rings and Climate*; Academic Press: London, UK, 1976.
27. Wigley, T.M.L.; Briffa, K.R.; Jones, P.D. On the average value of correlated time series, with applications in dendroclimatology and hydrometeorology. *J. Clim. Appl. Meteorol.* **1984**, *23*, 201–213. [\[CrossRef\]](#)
28. Osborn, T.J.; Briffa, K.R.; Jones, P.D. Adjusting variance for sample size in tree-ring chronologies and other regional mean time series. *Dendrochronologia* **1997**, *15*, 89–99.
29. Li, J.; Wu, Z.; Jiang, Z.; He, J. Can Global Warming Strengthen the East Asian Summer Monsoon? *J. Clim.* **2010**, *23*, 6696–6705. [\[CrossRef\]](#)
30. Rayner, N.A.; Horton, E.B.; Rowell, D.P.; Kent, E.; Parker, D.E.; Folland, C.K.; Alexander, L.; Kaplan, A. Global analyses of sea surface temperature, sea ice, and night marine air temperature since the late nineteenth century. *J. Geophys. Res.* **2003**, *108*, 4407. [\[CrossRef\]](#)
31. Li, F.; Chen, D.; Tang, Q. Variations of hydro-meteorological variables in the Yellow River basin and their relationships with the East Asian summer monsoon. *Adv. Water Sci.* **2015**, *26*, 481–490.
32. He, H.; Zhang, Q.; Zhou, J.; Fei, J.; Xie, X. Coupling climate change with hydrological dynamic in Qinling Mountains, China. *Clim. Chang.* **2008**, *94*, 409–427. [\[CrossRef\]](#)
33. Tan, L.; Cai, Y.; Cheng, H.; Edwards, L.R.; Gao, Y.; Xu, H.; Zhang, Z.; An, Z. Centennial- to decadal-scale monsoon precipitation variations in the upper Hanjiang River region, China over the past 6650 years. *Earth Planet. Sci. Lett.* **2018**, *482*, 580–590. [\[CrossRef\]](#)
34. Chen, F.; Yuan, Y.-J.; Wei, W.-S.; Fan, Z.-A.; Yu, S.-L.; Zhang, T.; Zhang, R.; Shang, H.; Qin, L. Reconstructed precipitation for the north-central China over the past 380 years and its linkages to East Asian summer monsoon variability. *Quat. Int.* **2013**, *283*, 36–45. [\[CrossRef\]](#)
35. Li, H.; Dai, A.; Zhou, T.; Lu, J. Responses of East Asian summer monsoon to historical SST and atmospheric forcing during 1950–2000. *Clim. Dyn.* **2010**, *34*, 501–514. [\[CrossRef\]](#)
36. Fang, K.; Gou, X.; Chen, F.; D’Arrigo, R.; Li, J. Tree-ring based drought reconstruction for the Guiling Mountain (China): Linkages to the Indian and Pacific Oceans. *Int. J. Clim.* **2009**, *30*, 1137–1145. [\[CrossRef\]](#)
37. Wang, L.; Qian, Y.; Zhang, Y.; Zhao, C.; Leung, L.R.; Huang, A.; Xiao, C. Observed variability of summer precipitation pattern and extreme events in East China associated with variations of the East Asian summer monsoon. *Int. J. Clim.* **2015**, *36*, 2942–2957. [\[CrossRef\]](#)
38. Wang, H. The weakening of the Asian monsoon circulation after the end of 1970’s. *Adv. Atmos. Sci.* **2001**, *18*, 376–386.
39. Zhai, J.; Su, B.; Krysanova, V.; Vetter, T.; Gao, C.; Jiang, T. Spatial Variation and Trends in PDSI and SPI Indices and Their Relation to Streamflow in 10 Large Regions of China. *J. Clim.* **2010**, *23*, 649–663. [\[CrossRef\]](#)
40. Liu, H.; Zhou, T.; Zhu, Y.; Lin, Y. The strengthening East Asia summer monsoon since the early 1990s. *Chin. Sci. Bull.* **2012**, *57*, 1553–1558. [\[CrossRef\]](#)
41. Chen, F.; Zhang, R.; Wang, H.; Qin, L. Recent climate warming of central China reflected by temperature-sensitive tree growth in the eastern Qinling Mountains and its linkages to the Pacific and Atlantic oceans. *J. Mt. Sci.* **2015**, *12*, 396–403. [\[CrossRef\]](#)
42. Ren, L.; Wang, M.; Li, C.; Zhang, W. Impacts of human activity on river runoff in the northern area of China. *J. Hydrol.* **2002**, *261*, 204–217. [\[CrossRef\]](#)
43. Liu, C.; Zhang, X. Causal analysis on actual water flow reduction in the mainstream of the Yellow River. *Acta Geogr. Sinica* **2004**, *59*, 323–330. (In Chinese)
44. Zheng, J.; Xiao, L.; Fang, X.; Hao, Z.; Ge, Q.; Li, B. How climate change impacted the collapse of the Ming dynasty. *Clim. Chang.* **2014**, *127*, 169–182. [\[CrossRef\]](#)
45. Chen, Z.; Yang, G. Analysis of drought hazards in North China: Distribution and interpretation. *Nat. Hazards* **2012**, *65*, 279–294. [\[CrossRef\]](#)

46. Hao, Z.; Zheng, J.; Wu, G.; Zhang, X.; Ge, Q. 1876–1878 severe drought in North China: Facts, impacts and climatic background. *Chin. Sci. Bull.* **2010**, *55*, 3001–3007. [[CrossRef](#)]
47. Zhu, Z.; Giordano, M.; Cai, X.; Molden, D. The Yellow River Basin: Water Accounting, Water Accounts, and Current Issues. *Water Int.* **2004**, *29*, 2–10. [[CrossRef](#)]
48. Huang, J.; Zhai, J.; Jiang, T.; Wang, Y.; Li, X.; Wang, R.; Xiong, M.; Su, B.; Fischer, T. Analysis of future drought characteristics in China using the regional climate model CCLM. *Clim. Dyn.* **2017**, *50*, 507–525. [[CrossRef](#)]
49. Sternberg, T. Chinese drought, bread and the Arab Spring. *Appl. Geogr.* **2012**, *34*, 519–524. [[CrossRef](#)]



© 2020 by the authors. Licensee MDPI, Basel, Switzerland. This article is an open access article distributed under the terms and conditions of the Creative Commons Attribution (CC BY) license (<http://creativecommons.org/licenses/by/4.0/>).